
Article

Impedance Spectroscopy and Conductivity Studies of NdCrO₃ Perovskite Ceramic Nanoparticles

Jada Shanker¹, M. Buchi Suresh² and D. Suresh Babu¹

¹Department of Physics, Osmania University, Hyderabad, Telangana, India

²International Advanced Research Centre for powder metallurgy and New Materials (ARCI) Hyderabad, India;

Abstract

Impedance, dielectric constant and conductivity properties of NdCrO₃ perovskite ceramics in a wide frequency range (1Hz -10MHz) with different temperatures have been studied. Sol-gel auto-combustion technique was used for synthesis NdCrO₃ Perovskite material. The Structural analysis of the NdCrO₃ ceramic sample has been confirmed as single phase orthorhombic structure by X-ray Diffractometer. The grains are uniformly distributed throughout the surface has been confirmed from the Microstructure of the NdCrO₃ sintered pellet. The Impedance, dielectric constant and conductivity properties of the NdCrO₃ Pervoskite compound have been investigated by using Impedance spectroscopy. The presence of grain and grain boundary effects in the material has been analyzed. The frequency variation electrical data were used to study the conductivity mechanism in the material. The analysis of the electrical Impedance, Dielectric constant and AC Conductivity with frequency at different temperatures has provided some information to support suggested conduction mechanism.

Introduction

The Pervoskite structure (ABO₃) compounds containing rare-earth (A), transition-metal (B) ions. The ABO₃ type Perovskite materials were exhibited important properties such as high temperature (T_c) superconductivity, colossal magneto resistance and multi ferocity [1-2]. The Orthochromatics with a common formula RCrO₃ investigated for their applications in various devices such as solid-oxide fuel cells and catalytic converters. NdCrO₃ is a good candidate for interconnect in high-temperature SOFCs because of their high electrical conductivity, high densification and good chemical stability [2]. In the recent years RCrO₃ type of materials exhibited a so called giant dielectric constant (ϵ') [3]. A literature survey of this material found to be there is no detailed work has

Received on
3rd March 2021

Revised on
9th May 2021

Accepted on
18th August 2021

been reported on the temperature and frequency dependence of electrical properties. Therefore, we have extensively studied the frequency and temperature dependence of dielectric and impedance properties of NdCrO_3 perovskite ceramics. This paper has presented our extensive investigations on electrical properties of NdCrO_3 .

Experimental procedure

Polycrystalline powder of NdCrO_3 was prepared by sol-gel auto combustion technique. The required chemicals for NdCrO_3 synthesis are presented in **table 1**. For making NdCrO_3 we have taken 1:1 molar ratio of Stoichiometric amounts of Nd_2O_3 and $\text{Cr}(\text{NO}_3)_3 \cdot 9\text{H}_2\text{O}$ and 1:3 molar ratio of citric acid was taken separately. Nd_2O_3 is converted as neodymium nitrate using HNO_3 . This weighted raw materials has been dissolved individually by using double distilled water, and mixed using magnetic stirrer for homogeneous solution, then the PH value of mixed solution has been set to 7 by adding of NH_3 . This mixed solution was stirred and simultaneously heated to 150°C to evaporate water and until the sole was obtained, then ethylene glycol was added as a fuel. The resulting gel was combusted. Collected powders were annealed (calcined) at 750°C for 4h. The obtained powder was pressed into pelletized under uniaxial pressing. The pellets were sintered individually at 900°C temperature. Finally, these sintered pellets were used for SEM and dielectric measurements.

Phase and Crystallographic structure of the NdCrO_3 Pervoskite has been characterized by SHIMADZU XRD-7000 X-Ray Diffractometer (XRD), in this technique monochromatic Cu K radiation used as Phase detector. Microstructure and the grain size distribution of the sintered pellet were studied using a Scanning Electron Microscope (SEM) ZISS EVO-18. NdCrO_3 density was calculated by using the Archimedes principle and also measuring the mass and volume of the pellets and comparing them to that expected from the theoretical X-ray density. The SOLARTRON SI1260 model Impedance analyzer was used to carry out dielectric and impedance spectroscopic measurements. The silver electrode coated surfaces of the 10mm diameter and 2mm thickness of circular shape of pellets has been used for the dielectric measurements.

Results and Discussion

Material characterization

XRD pattern of annealed (calcined) powder of NdCrO_3 is shown in **Figure 1**. XRD was refined by using Rietveld refinement FullProf Suite program (2.05) July 2011 version software. The evaluated lattice parameters and refinement parameter are given in **Table 2**. It has been suggested that the material has single phase orthorhombic symmetry. The grain size calculated using Scherer formula and is found to be 31.9nm.

Figure 2 shows the grain size, grain distribution and voids of NdCrO_3 sintered pellet have been found in surface morphology of the SEM microstructure. The grains are systematically distributed around the surface and the average grain size is found to be an order of 100nm. The SEM microstructure shows that the varying grain sizes of well-defined grain boundaries of morphology reveals the NdCrO_3 is Polycrystalline nature [4]. The density of the pellet has calculated and is found to be around 94%. The very less no. of voids are observed in the compound, it indicates that the pellet has a certain amount of porosity.

Dielectric measurements

The frequency variation dielectric constant (ϵ') of NdCrO_3 at various temperatures has shown in **Figure 3**. It has found that the dielectric constant (ϵ') decreases with rising frequency for all given

temperatures. The dielectric constant (ϵ') found to be increased with increasing temperature, which becomes even more significant at low frequency. The dielectric constant (ϵ') found to be high value in the low frequency region, and is decreasing with rising frequency is due to the space charges polarization, which leads to the high dielectric constant and significant frequency dispersion [5-7]. This suggests that the thermally activated nature of the dielectric relaxation occurs in the NdCrO₃ material [7].

The frequency dependent dielectric loss ($\tan\delta$) of NdCrO₃ Pervoskite ceramic at different temperatures has shown in **Figure 4**. It shows that dielectric loss ($\tan\delta$) decreases with rising frequency at a given temperature. As the increasing temperature, the dielectric loss ($\tan\delta$) increases below the 175^oC in the low frequency region due strong space charge polarization and then it decreases with increasing temperature may be due to weak space charge polarization in the material [8]. The dielectric loss becomes even more significant at low frequency. The high value of dielectric loss ($\tan\delta$) observed in the low frequency region, it is corresponding to low conductivity of the grain boundary. In the high frequency region loss is constant, indicates high conductivity of grain [9].

Impedance measurements

The **Figure 5** shown that frequency dependence real part impedance (Z') of NdCrO₃ at various temperatures has shown in **Figure 5**. The real part impedance (Z') has shown higher value at lower temperature in the low frequency region, and is gradually decreased with the rise in frequency and temperature. The real part impedance (Z') value of all temperatures has merged in the high frequency region. The decrease in Z' value with increasing frequency is may be due to the possibility of an increase in AC conductivity (σ_{ac}) with the rise in frequency. In the high frequency region real part impedance (Z') at all temperatures were merged, it is due to the possible release of space charge and a consequent lowering the barrier properties of NdCrO₃ Pervoskite material [10-12].

The **Figure 6** shows that the frequency dependence of imaginary impedance (Z'') of NdCrO₃ Pervoskite at different temperatures is shown in **Figure 6**. The two peaks are observed in each curve one at a high frequency region (shown in inset) and the other at low frequency region, indicating two relaxations corresponding to grain and grain boundary conduction respectively [13]. Both the peaks are shifting to the high frequency side on increasing temperature, and then a strong dispersion of Z'' exists. The variation of peak frequency shifting in Z'' with the rise in frequency and temperature, it is due to the presence of an electrical relaxation phenomenon in the NdCrO₃ Pervoskite material, and is clear proof of temperature dependent relaxation. The heights of peaks are found to decrease gradually with the increase in frequency. The full width half maxima of the peak points indicates the possibility of a distribution of relaxation times. This relaxation time (τ) was calculated from the position of the peak using the relation [7].

$$\tau = \frac{1}{\omega_{max}}$$

Figure 7 Shows the Cole-Cole plot (Z' Vs Z'') of NdCrO₃ Perovskite ceramic at different temperatures. The impedance of the NdCrO₃ Perovskite ceramic material grows into apparently visible with rise in temperature. An increasing temperature, the slope of the line decreases, i.e. they bend towards Z' axis and finally forms semicircles. The existence of two arcs or semicircles at an appropriate temperature shows the electrical properties of the materials emerge mainly due to the contribution of the grain and grain boundary property in the NdCrO₃ Perovskite ceramic material. The construction of full, partial or no semicircles in the NdCrO₃ Perovskite ceramic material may be due to the strength of

relaxation and also experimentally available frequency range [14]. The electrical process taking place within the NdCrO₃ Perovskite ceramic material may be modelled (RC circuit), it works on the basis of the bricklayer model. The intercept of the semicircle on Z'-axis gives the value of grain (bulk) resistance (R_g) and grain (R_{gb}) resistance of the sample respectively. R_g and R_{gb} value decreased with increasing temperature. It suggests that material shows the negative temperature coefficient of resistance (NTCR) type behavior. These plots show depressed semicircles may be due to the existence of the non-Debye type of relaxation phenomenon in the materials [14].

Z''/Z''_{max} Vs f/f_{max} plots of NdCrO₃ perovskite ceramic material has been presented in **Figure 8**. The full width half maxima (FWHM) is found to be more than 1.14 decades, this behavior suggests the relaxation in NdCrO₃ perovskite ceramic material is non-Debye type [15], supporting previous discussions.

Figure 9 shows the variation of the relaxation time (τ) of grain and grain boundary as a function of temperature. The relaxation time (τ) follows the Arrhenius law.

$$\tau = \tau_0 \exp\left(\frac{E_a}{K_b T}\right).$$

Where E_a is activation energy, K_b is boltzman constant, τ_0 is pre – exponential factor

The typical pattern reveals that the temperature dependent relaxation process with a spread of relaxation time suggesting enhancement in the process dynamics in the NdCrO₃ perovskite ceramic material with the rise in temperature [7]. The activation energies estimated for grain and grain boundary relaxation time and are found to be $E_{a(g\tau)} = 0.75eV$ and $E_{a(gb\tau)} = 0.53eV$.

DC & AC Conductivity analysis

Figure 10 Shows the Grain and grain boundary [inset] DC conductivity $V_s 10^3/T$ plot of NdCrO₃. It observed that the a pattern of DC conductivity increases gradually with increasing temperature, suggesting a thermally activated process in the NdCrO₃ perovskite ceramic material [7]. The value of grain and grain boundary DC conductivity has been calculated from the impedance data using the relation.

$$\sigma_{dc} = \frac{t}{RA}$$

Where R is the grain or grain boundary resistance, t is the thickness, and A is the area of the electrode deposited on the sample.

The DC conductivity of bulk (grain) and grain boundary follow the Arrhenius law. The activation energies of DC conductivity for grain and grain boundaries of NdCrO₃ perovskite ceramic material, are evaluated and are found to be $E_{a(gdc)} = 0.6eV$ and $E_{a(gbdc)} = 0.71eV$.

Figure 11 Shows frequency dependence AC conductivity plots of NdCrO₃ Perovskite for various temperatures. The AC conductivity of the sample was evaluated by using the formula.

$$\sigma_{ac} = 2\pi f \epsilon_0 \epsilon' \tan \delta$$

Where f =frequency, $\tan\delta$ = dielectric loss, ϵ_0 =dielectric constant in free space, ϵ' =dielectric constant.

The AC conductivity (σ_{ac}) Remained constant (plateau region) at lower frequencies and increased rapidly with increasing temperature at higher frequencies, which may be due to the increase in the number of charge carriers and their drifted mobility which are thermally activated in NdCrO₃ perovskite ceramic material [16].

The DC conductivity (σ_{dc}), frequency coefficient (A) and frequency exponent (n) were calculated from the low frequency curve of (σ_{ac} Vs f) plot by using Jonscher’s law relation and given in **table. 3** .The hopping frequency (ω_p) obtained at the point where the slope changes in the conductivity spectrum. The conductivity curves of the NdCrO₃ perovskite ceramic material follow the Jonscher’s power law [17].

$$\sigma_{ac} = \sigma_{dc} + A\omega^n$$

Where n is the frequency exponent in the range of $0 \leq n \leq 1$.

The plateau region of the plot corresponds to the frequency independent part DC conductivity (σ_{dc}), and Dispersive region corresponds to the frequency dependent part ($A\omega^n$). The increases in conductivity with temperature reveals that the electrical conduction in the material is a thermally activated process [7].

Table 1. Required Chemicals to Synthesis of NdCrO₃.

Chemical Name	Molecular weight	Purity (%)	Grade	Make
Nd ₂ O ₃	336.477	99.99	-	Indian rare earth
HNO ₃	63.01	69	AR	SD Fine
Cr(NO ₃) ₃ .9H ₂ O	400.15	98	GR	LOBA
C ₆ H ₈ O ₇ .H ₂ O	210.14	99.5	GR	MARK
NH ₃	17.03	25	AR	SD Fine
C ₂ H ₆ O ₂	62.07	99	AR	SD Fine

Table 2 Lattice parameters and Rietveld refinement parameters of NdCrO₃ calcined powder

Lattice parameters (Å ⁰)	a	5.482(2)
	b	7.694(2)
	c	5.424(3)
Rietveld refinement parameters	Profile (R _p)	6.2
	Weighted profile (R _{wp})	5.7
	Expected (R _{EXP})	7.5
	Goodness of fit (S)	1.4
Structure	Orthorhombic	Pnma

Table 3 Johnson power law parameters of NdCrO3 sintered pellet

Temperature (°C)	σ_{dc}	A	ω	n
RT	0.0006	4E-7	25924	0.92
50	0.0007	3E-7	39935	0.95
75	0.0011	3E-7	64679	0.958
100	0.0026	2E-7	66231	0.985
125	0.0040	3E-7	64716	0.953
150	0.0074	1E-6	16009	0.885
175	0.0110	2E-7	10191	1.000
200	0.0102	2E-6	4040	0.874
225	0.0080	1E-6	6283	0.965
250	0.0073	2E-6	6408	0.910
275	0.0085	1E-6	6283	0.955
300	0.0121	8E-7	4084	0.970

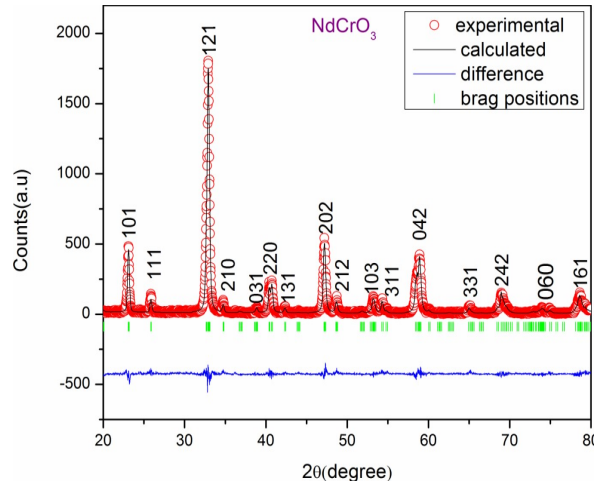


Figure 1: XRD-Rietveld refinement of annealed powder of NdCrO3. Open circles represent experimental data and solid curve shows a calculated pattern. The curve below the straight line gives the difference between the experimental and calculated pattern, vertical pattern lines indicate the bragg positions.

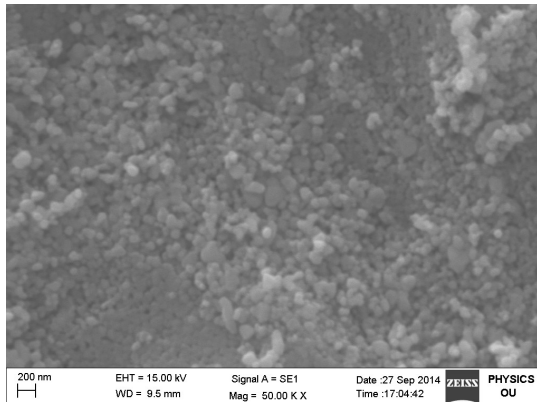


Figure 2: Scanning electron microscopy (SEM) Microstructure of sintered pellet of NdCrO3

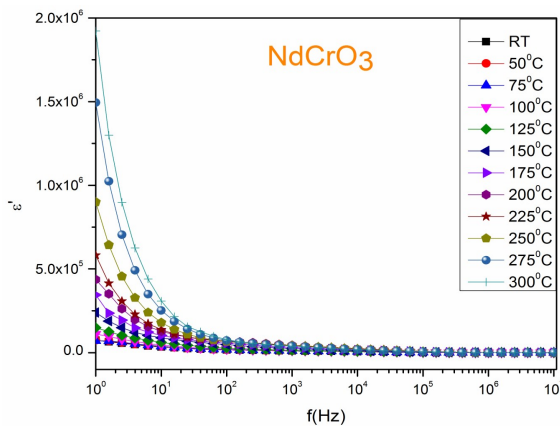


Figure 3: Frequency dependence of the dielectric constant (ϵ') of NdCrO3 at different temperatures

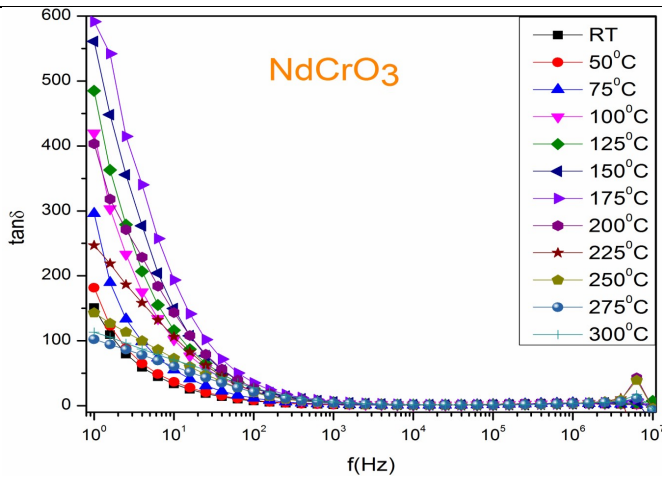


Figure 4: Frequency dependence of the dielectric loss ($\tan\delta$) of NdCrO₃ at different temperatures.

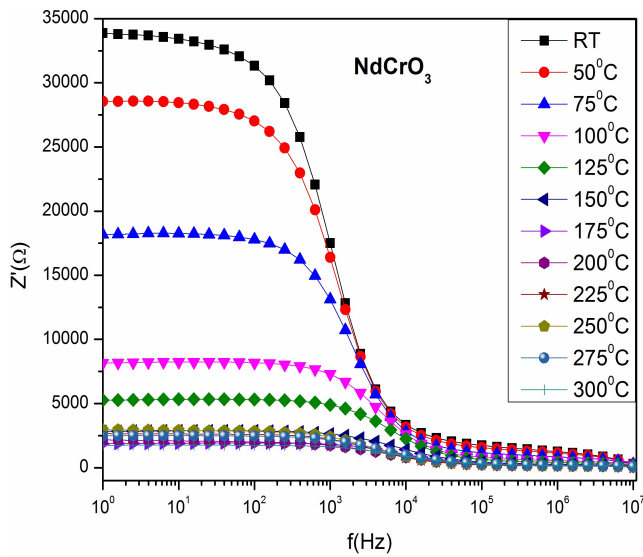


Figure 5: Frequency dependence of Real part impedance (Z') of NdCrO₃ at different temperatures

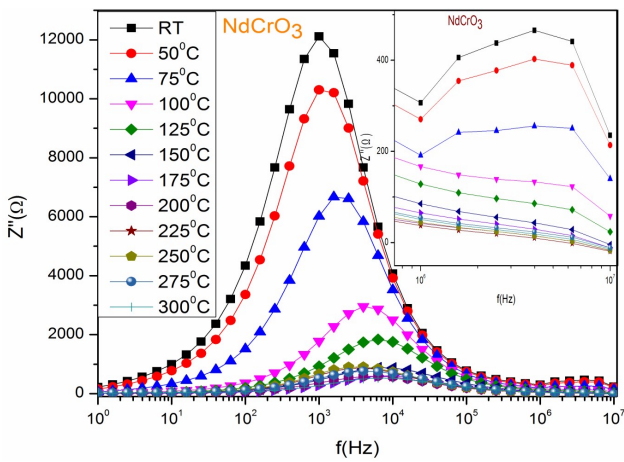


Figure 6: Frequency dependence of imaginary impedance (Z'') of NdCrO₃ at different temperatures. Inset shows zoom view of the high frequency region

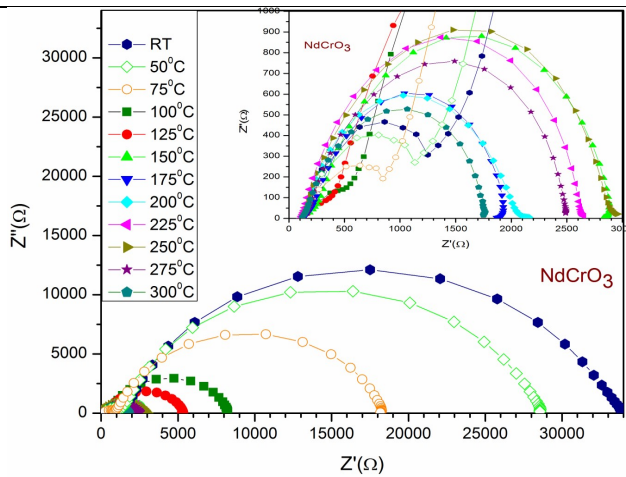


Figure 7: Complex impedance spectrum Z' Vs Z'' (Cole-Cole plot) of NdCrO_3 at different temperatures. Inset set fig shows zoom view of the high frequency region (grain)

Coding in the Two-stage Scheme

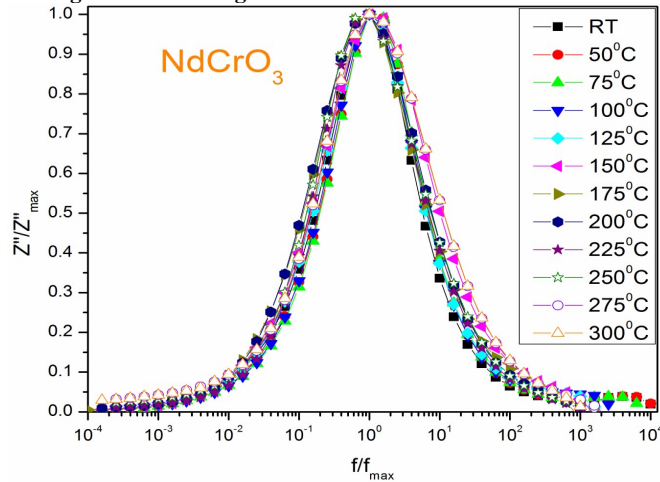


Figure 8: Z''/Z''_{\max} Vs f/f_{\max} plots of NdCrO_3 at different temperatures

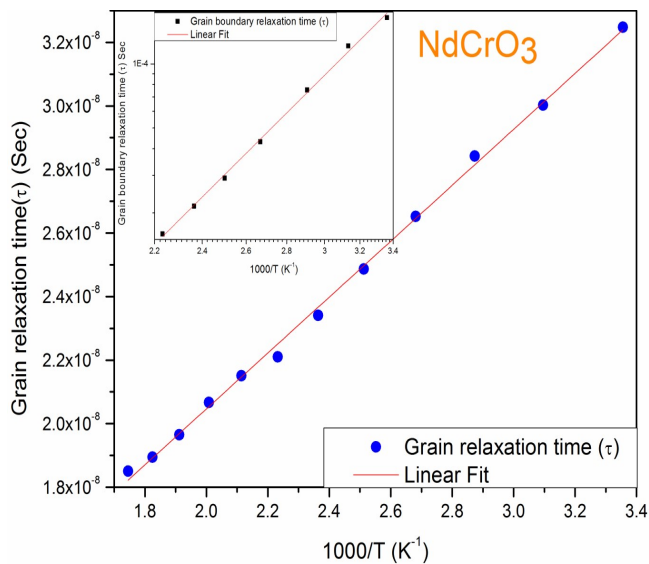


Figure 9: Variation of grain and grain boundary [insert] relaxation time (τ) of NdCrO_3 as a function of temperature

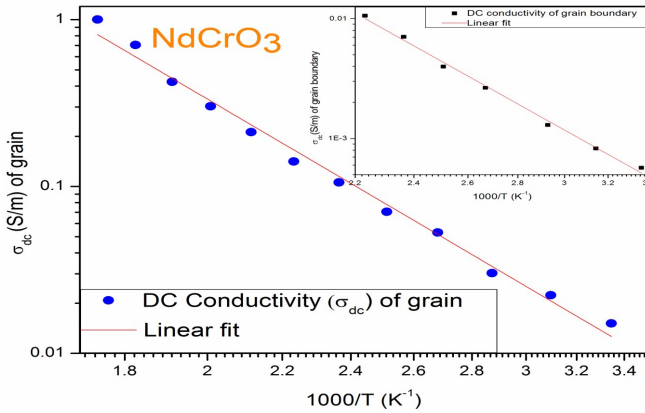


Figure 10: Variation of DC conductivity (σ_{dc}) of grain and grain boundary [insert] of NdCrO3 as a function of temperature

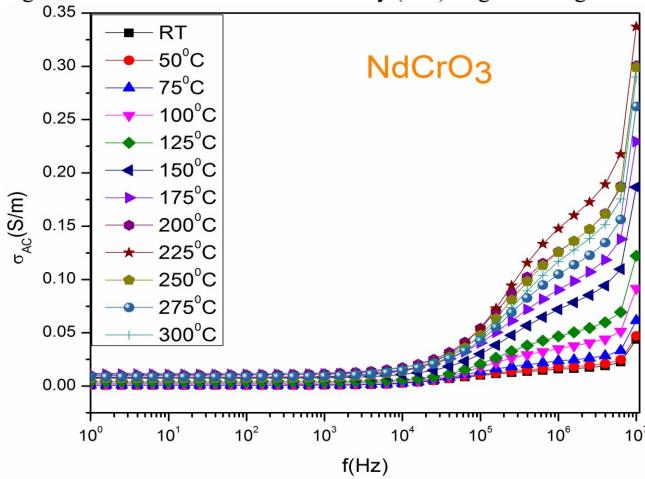


Figure 11: Frequency dependence AC conductivity (σ_{ac}) Plots of NdCrO3 at different temperatures

Conclusions

The NdCrO₃ perovskite ceramic sample was prepared by Solgel Autocombustion technique. The phase formation of the NdCrO₃ perovskite ceramic sample was confirmed by XRD, it is a single phase orthorhombic structure. The Activation energies of DC conductivity (σ_{dc}), relaxation time (τ) of grain and grain boundaries has evaluated, and were followed the Arrhenius law. The real and imaginary parts of impedance properties for NdCrO₃ perovskite ceramic sample has investigated. The impedance analysis indicates that the typical behavior of negative temperature coefficient of resistance (NTCR) of NdCrO₃ perovskite ceramic materials. Further, it also confirmed the presence of non-Debye type relaxation phenomenon observed in the material. The increase in AC conductivity with increasing temperature may be due to the increase in the number of charge carriers and their drifted mobility which are thermally activated. Frequency dependent conductivity follows the Jonscher's law and at higher frequencies the hopping conduction increases.

Note

A Part of this work is presented at National conference on Physics and Chemistry of Solids at Department of Physics, SR & BGNR Govt Arts & Science College, Khammam.

References

- [1] Yi Du, Zhen Xiang Cheng, Xiao-Lin Wang, and Shi Xue Dou "Structure, magnetic, and thermal properties of $\text{Nd}_{1-x}\text{La}_x\text{CrO}_3$ ($0 \leq x \leq 1$)" JOURNAL OF APPLIED PHYSICS 108, 093914 (2010)
- [2] Yu Shen, Monan Liu, and Tianmin He, San Ping Jiang. "Preparation, Electrical Conductivity, and Thermal Expansion Behavior of Dense $\text{Nd}_{1-x}\text{Ca}_x\text{CrO}_3$ Solid solutions" J. Am. Ceram. Soc.92 [10] 2259-2264 (2009).
- [3] Bandi Vittal Prasad, G.Narsinga Rao, J.W. Chen, D. Suresh Babu. "Relaxor Ferroelectric like giant Permittivity in PrCrO_3 semiconductor ceramics" Materials Chemistry and Physics 126 (2011)918-921.
- [4] H.O. Rodrigues, G.F.M. Pires Junior, J.S. Almeida, E.O. Sancho, A.C. Ferreira, M.A.S. Silva, A.S.B. Sombra. "Study of the structural, dielectric and magnetic properties of Bi_2O_3 and PbO addition on BiFeO_3 ceramic matrix" Journal of Physics and Chemistry of Solids 71(2010) 1329-1336
- [5] N. K. Singh, Pritam Kumar, Hemchand Kumar, Radheshyam Rai "Structural and dielectric properties of $\text{Dy}_2(\text{Ba}_{0.5}\text{R}_{0.5})_2\text{O}_7$ (R=W, Mo) ceramics" Adv. Mat. Let. 2010,1 (1),79-82
- [6] S. Sreehari Sastry, L. Tanuj Kumar, and Ha Sie Tiong "Dielectric Studies on Benzothiazole Based Liquid Crystals at Radio Frequency Region" International Journal of Innovative Research in Science, Engineering and Technology, Vol. 3, Issue 3, March 2014 ,10212-10219
- [7] Subrat K. Barik, R.N.P. Choudhary, A.K. Singh "AC impedance spectroscopy and conductivity studies of $\text{Ba}_{0.8}\text{Sr}_{0.2}\text{TiO}_3$ ceramics" Adv. Mat. Let. 2011,2(6),419-424.
- [8] Shrivastav B.D., Barde R., Mishra A. And Phadake S. "Frequency and Temperature Dependence of Dielectric Properties of Fish Scales Tissues" *Research Journal of Physical Sciences*, Vol. 1 (6), 24-29, July (2013) *Res. J. Physical Sci.*
- [9] Navneet Sing, Ashish Agarwal, Sujata Sanghi. "Dielectric relaxation, conductivity behavior and magnetic properties of Mg Substituted Zn-Li ferrites" Current Applied Physics 11 (2011) 783-789.
- [10] Hemant Singh, Amit Kumar, K.L. Yadav, "Structural, dielectric, magnetic, magnetodielectric and impedance spectroscopic studies of multiferroic BiFeO_3 - BaTiO_3 ceramics" Materials Science and Engineering B 176 (2011) 540-547.
- [11] Archana Shukla, R.N.P. Choudhary, "Impedance and modulus spectroscopy characterization of $\text{La}_{1/3}\text{Mn}_{1/3}\text{O}_3$ modified PbTiO_3 nanoceramics" Current Applied Physics 11 (2011) 414-422.
- [12] Balgovind Tiwari, R.N.P. Choudhary, "Frequency-temperature response of $\text{Pb}(\text{Zr}_{0.65-x}\text{Ce}_x\text{Ti}_{0.35})\text{O}_3$ ferroelectric ceramics: Impedance spectroscopic studies" Journal of Alloys and Compounds 493 (2010) 1-10
- [13] S. A. Acharya, K. Singh "Grain shape effect on dielectric properties and ionic Conductivity of Gd-doped ceria" Adv. Mat. Let. 2014, 5(2), 61-66.
- [14] Rajiv Ranjan, Nawnit Kumar, Banarji Behera, R. N. P. Choudhary, "Investigation of impedance and electric modulus properties of $\text{Pb}_{1-x}\text{Sm}_x(\text{Zr}_{0.45}\text{Ti}_{0.55})_{1-x/4}\text{O}_3$ ceramics" Adv. Mat. Let. 2014, 5(3),138-142.
- [15] N. V. Prasad, M. Chandra Sekhar & G. S. Kumar "Impedance Spectroscopic Studies on Lead Based Perovskite Materials" *Ferroelectrics*, 366:1, 55-66.
- [16] Khalid Sultan, M. Ikram, K. Asokan "Structural, optical and dielectric studies of Mn doped PrFeO_3 ceramics" Vacuum 99 (2014) 251-258.
- [17]. A. K. Jonscher "The 'universal' dielectric response" Nature Vol. 267, 673-679, 23, Jun 1977.